

The Fundamental Plane of Black Hole Activity Represented in Terms of Dimensionless Beam Power and Bolometric Luminosity

Ruth. A. Daly^{*}, Douglas A. Stout, and Jeremy N. Mysliwiec

Penn State University, Berks Campus, Reading, PA 19608, USA

2 August 2016

ABSTRACT

The fundamental plane (FP) of black hole activity indicates a relationship between compact radio emission, X-ray luminosity, and black hole mass of black hole systems. The plane is thought to be a manifestation of an underlying relationship between jet power, L_j , bolometric accretion disk luminosity, L_{bol} , and black hole mass (or Eddington luminosity, L_{Edd}) with compact radio emission related to jet power and X-ray emission related to disk luminosity. It is shown here that the FP may be recast in the dimensionless form $\log(L_j/L_{Edd}) = A \log(L_{bol}/L_{Edd}) + B$, where A can be expressed in terms of best fit FP parameters. This representation allows comparisons between sources with a variety of tracers of beam power and disk luminosity and elucidates the relationship between L_j , L_{bol} and L_{Edd} . Consistent values of A are obtained for nine samples of sources. Samples of LINERS, AGN, and XRB that lie on the FP are converted to dimensionless luminosities and studied and a sample of FRII radio sources with known values of L_j , L_{bol} and L_{Edd} is included; the dimensionless fundamental plane has a smaller dispersion than the FP supporting the original interpretation of the FP. The results and implications are discussed.

Key words: black hole physics – galaxies: active

1 INTRODUCTION

The fundamental plane (FP) of black hole activity was introduced and studied extensively by Merloni, Heinz, & Di Matteo (2003) and Falcke, Körding, & Markoff (2004). Subsequently, the FP has been studied with additional sources by many groups including Körding, Falcke, & Corbel (2006), Gültekin et al. (2009), Bonchi et al. (2013), Saikia, Körding, & Falcke (2015), and Nisbet & Best (2016), hereafter NB16. The fundamental plane encapsulates the relationship between compact radio luminosity, X-ray luminosity, and black hole mass for black hole systems and provides a good description of the data over a very large range of black hole mass. As has been discussed by many authors, such as Heinz & Sunyaev (2003), Merloni et al. (2003), Falcke et al. (2004), Körding, Fender, & Migliari (2006), Merloni & Heinz (2007), Fender (2010), de Gasperin et al. (2011), and Saikia, Körding, & Falcke (2015), to name a few, the radio and X-ray powers or luminosities are likely to be related to two fundamental physical variables, the beam power and bolometric luminosity of the accretion disk, that describe the system. The radio power L_R is likely to be related to

the beam power, L_j , of an outflow, with $L_j \propto L_R^\alpha$, where the beam power of the outflow is defined as the energy per unit time, dE/dt ejected by the source in some form such as bulk kinetic energy, and the X-ray luminosity is likely to be related to the bolometric luminosity, L_{bol} , of the accretion disk, with $L_{bol} \propto L_X(2 - 10 \text{ keV})$. In addition, Saikia et al. (2015) introduce the bolometric FP that replaces L_X with L_{bol} where L_{bol} is obtained from the OIII luminosity of sources.

Many black hole systems may not have measured compact radio emission or X-ray emission yet may have bolometric luminosity and beam power estimates obtained using other tracers. To determine whether the relationship between outflow properties, accretion disk properties, and black hole mass or Eddington luminosity are consistent with those indicated by the FP of black hole activity, it is helpful to see if the FP may be rewritten in terms of other parameters such as dimensionless beam power and dimensionless bolometric luminosity. The fact that the FP is valid over a very large black hole mass range suggests that it can be written in terms of dimensionless luminosities. With this representation, more sources can be compared, and the range of values of dimensionless beam power and dimensionless bolometric luminosity and the relationship between these quan-

^{*} E-mail: rdaly@psu.edu

tities can be studied. The question of whether the FP can be recast in dimensionless form is addressed in section 2. Applications to data sets to obtain dimensionless luminosities are presented in section 3. The results are summarized and discussed in section 4.

2 ANALYSIS

The FP plane of black hole activity may be written in a few different forms. Following NB16, we consider the form

$$\log L_R = a \log L_{X,42} + b \log M_8 + c, \quad (1)$$

where L_R is the 1.4 GHz radio power of the compact radio source in erg s^{-1} , $L_{X,42}$ is the (2 - 10) keV X-ray luminosity of the source in units of $10^{42} \text{ erg s}^{-1}$, and M_8 is the black hole mass in units of $10^8 M_\odot$; conversions to other wavebands are discussed by NB16. NB16 present results obtained with a sample of 576 LINERS and summarize results obtained by Merloni et al. (2003), K rding et al. (2006), G ltekin et al. (2009), Bonchi et al. (2013), and Saikia et al. (2015).

Sources with a huge range of black hole mass, about nine orders of magnitude, follow this relation, suggesting that the relationship between the fundamental physical variables L_j , L_{bol} , and black hole mass M scale in such a way that the overall relationship is maintained. If the equation that describes the relationship between fundamental physical variables is written in terms of dimensionless quantities then it is scale-invariant and we expect the relationship to remain valid for all scales. The simplest equation written in terms of dimensionless quantities with a form similar to that of the fundamental plane is

$$\log \left(\frac{L_j}{L_{Edd}} \right) = A \log \left(\frac{L_{bol}}{L_{Edd}} \right) + B, \quad (2)$$

where L_{Edd} is the Eddington luminosity, $L_{Edd} \simeq 1.3 \times 10^{46} M_8 \text{ erg s}^{-1}$, and A and B are constants. So, the goal is to determine whether the FP [eq. (1)] can be written in this form.

As described in section I, it is convenient to write the bolometric luminosity of the accretion disk as

$$L_{bol} = \kappa_X L_X(2 - 10 \text{ keV}) \quad (3)$$

and the beam power L_j as

$$\log L_j = C \log L_R + D, \quad (4)$$

where L_{bol} , $L_X(2 - 10 \text{ keV})$, L_j and L_R are in erg s^{-1} . Substituting eqs. (3) and (4) into eq. (1) indicates that

$$\log \left(\frac{L_j}{L_{Edd}} \right) = aC \log L_{bol} - (1 - bC) \log L_{Edd} + \kappa \quad (5)$$

where $\kappa = D + C(c - 42a - 46.11b - a \log \kappa_X)$.

Eq. (5) may be written in the form of eq. (2) when $aC = (1 - bC)$; that is, when $C = (a + b)^{-1}$. Three approaches are used to determine whether this is satisfied. First, C is computed using $C = (a + b)^{-1}$, and the values obtained for different data sets are shown to be consistent. The values are compared with that expected based on theoretical studies and based on independent studies of radio sources, and it is shown that there is good agreement between the empirical values, $C = (a + b)^{-1}$, theoretically predicted values, and values based on independent studies of radio sources. Second, the values of aC and $(1 - bC)$ are computed using the

value of C indicated by theoretical studies and by independent studies of radio sources, and the difference between aC and $(1 - bC)$ is shown to be consistent with zero. And, third, again using the value of C indicated by theoretical studies and by independent studies of radio sources, the ratio of aC to $(1 - bC)$ is computed and is shown to be consistent with unity. These results indicate that aC is equal to $(1 - bC)$ and thus eq. (1) may be written in the form of eq. (2). Details of the analysis just described are presented in section 2.1 and are summarized in section 2.2.

2.1 Details of the Analysis

The values of $C = 1/(a+b)$ are listed in Table 1 for the values of a and b summarized in Table 1 of NB16. The nine values of C obtained are all consistent; they range from about 0.61 to 0.93 with a median value of 0.72 and unweighted mean value of 0.74; all of the sources are within one sigma of these mean and median values, as expected based on the consistency of the values of a and b listed by NB16. As discussed below, the mean and median values of C are consistent with theoretical predictions and independent studies of radio sources.

An independent estimate of C , and an estimate of D , may be obtained by considering independent studies of radio sources. Using the relation between core radio luminosity and extended radio luminosity for radio galaxies presented by Yuan & Wang (2012) and applying the conversion of extended radio power to beam power presented by Willott et al. (1999), we obtain $C = 0.71 \pm 0.03$ and $D = 14.2 \pm 1.0$; radio galaxies are used rather than radio loud quasars since in this case the core radio emission is expected to have minimal effects due to relativistic beaming in the direction of the observer. In detail, using the standard conversion of luminosity density L_ν to power P of $P = L_\nu \nu$, the luminosity densities described by Yuan & Wang (2012) are converted to radio powers, and the conversion factor of NB16 is used to convert 5 GHz radio power to 1.4 GHz radio power. The extended 408 MHz radio power is converted to 151 MHz total power assuming a standard radio spectral index of -0.7 for the extended emission; note that the correction factor is very small because the frequencies (e.g. 408 and 151 MHz) are so similar. The extended radio power is converted to beam power using the relation presented by Willott et al. (1999) $L_j \simeq 1.7 \times 10^{45} f^{3/2} P_{44}^{6/7} \text{ erg s}^{-1}$, where P_{44} is the extended 151 MHz radio power in units of $10^{44} \text{ erg s}^{-1}$, and the factor f is expected to range between 1 and 20. Allowing for the full range of values of f and propagating all of the uncertainties, it turns out that the uncertainty of C is dominated by the uncertainty between core radio luminosity and extended radio luminosity, and that of D is dominated by the range of f .

Theoretical studies such as those by Heinz & Sunyaev (2003) and Merloni & Heinz (2007) indicate that the value of C is expected to be $12/17 \simeq 0.71$ when the radio spectral index of the compact radio source is close to zero. This agrees with the value of 0.71 ± 0.03 indicated by the independent studies of radio sources. The fact that the values of C indicated by the best fit values of a and b (see column 2 of Table 1) are consistent with that predicted theoretically and indicated by independent studies of radio sources suggests that relativistic beaming is likely to have a small effect on

Table 1. Study of Parameters

(1) Sample	(2) $C = \frac{1}{(a+b)}$	(3) aC	(4) $(1 - bC)$	(5) $aC - (1 - bC)$	(6) $\frac{aC}{(1-bC)}$	(7) $A = \frac{a}{(a+b)}$	(8) $B = \kappa$	(9) D
NB16(1) ^a	0.75 ± 0.07	0.46 ± 0.05	0.51 ± 0.07	-0.05 ± 0.09	0.90 ± 0.18	0.49 ± 0.05	-1.87 ± 2.09	14.93 ± 2.61
M03	0.72 ± 0.08	0.43 ± 0.08	0.45 ± 0.07	-0.02 ± 0.11	0.95 ± 0.25	0.43 ± 0.05	-2.80 ± 1.99	15.86 ± 3
K06	0.72 ± 0.26	0.45 ± 0.28	0.47 ± 0.21	-0.02 ± 0.36	0.96 ± 0.75	0.46 ± 0.19	-2.70 ± 2.03	15.76 ± 10.1
K06	0.74 ± 0.11	0.40 ± 0.05	0.45 ± 0.13	-0.04 ± 0.14	0.91 ± 0.30	0.42 ± 0.06	-2.52 ± 1.96	15.58 ± 4.03
G09	0.69 ± 0.14	0.48 ± 0.09	0.45 ± 0.19	0.03 ± 0.21	1.07 ± 0.51	0.46 ± 0.10	-3.90 ± 2.04	16.96 ± 5.43
G09	0.69 ± 0.06	0.44 ± 0.07	0.42 ± 0.06	0.02 ± 0.09	1.05 ± 0.25	0.43 ± 0.05	-3.88 ± 1.98	16.94 ± 2.38
B13	0.93 ± na	0.28 ± 0.04	0.52 ± na	-0.24 ± na	0.54 ± na	0.36 ± na	5.07 ± 1.86	7.99 ± na
S15	0.80 ± 0.29	0.45 ± 0.28	0.57 ± 0.14	-0.11 ± 0.32	0.80 ± 0.54	0.51 ± 0.18	na ± na	na ± na
S15	0.61 ± 0.13	0.59 ± 0.21	0.42 ± 0.14	0.17 ± 0.26	1.41 ± 0.71	0.50 ± 0.11	-7.58 ± 2.11	20.64 ± 5

^a All input values are from Table 3 of NB16, with the first line here corresponding to the first line of that Table. Other values follow in the same order as presented in Table 3 of NB16 beginning with Merloni et al. (2003) [M03]; K rding et al. (2006) [K06]; G ltekin et al. (2009) [G09]; Bonchi et al. (2013) [B13]; and Saikia et al. (2015) [S15].

the compact radio emission for most of the sources used to construct the fundamental plane.

To further test whether eq. (5) can be written in the form of eq. (2) the values of aC and $(1 - bC)$ and their difference and ratio is computed and listed in columns (3), (4), (5), and (6) of Table 1, where the value of C indicated above of 0.71 ± 0.03 is used to compute values for columns (3) through (6). The difference listed in column (5) is consistent with zero for all of the samples. And, the ratio $aC/(1 - bC)$ listed in column (6) is consistent with unity.

2.2 Summary of Analysis

These considerations indicate that eq. (1) may be written in the form of eq. (2), where $A = a/(a + b)$, $C = 1/(a + b)$, and $B = \kappa$. In terms of understanding the physics of the sources and constraining models that describe the sources, A is the most important parameter since eq. (2) implies that $L_j \propto L_{bol}^A M^{(1-A)}$. The parameter A may be obtained using best fit parameters to the fundamental plane, or by fitting to eq. (2). The value of A obtained from best fit values of a and b are listed in column (7) of Table 1 for nine samples of sources, and all values are consistent within the uncertainties. Values of A obtained from eq. (2) by fitting directly to dimensionless luminosities are discussed in section 3.

The normalization of the relationship is described by B . The value of B may be obtained from $B = \kappa$, which requires values of C , D , $\log \kappa_X$ as well as best fit values of a , b , and c . To compute B , the value of C listed in column (2) of Table 1 is used, as is $D = 14.2 \pm 1.0$ obtained as described above. To obtain an estimate for $\log \kappa_X$, the bolometric luminosity of each source with a measured (2-10 keV) X-ray luminosity listed by Merloni et al. (2003) was obtained using eq. (21) from Marconi et al. (2004); this indicates a mean value of $\log \kappa_X = 1.18 \pm 0.03$, which is in good agreement with the value obtained by Ho (2009). It is easy to show that propagating the uncertainties of all parameters, the uncertainty of c has an insignificant impact on the uncertainty of B , so this term is not included in computing the uncertainty of B . With these values, B is obtained and listed in column (8) of Table 1.

In addition, we may write $D = B - C(c - 42a - 46.11b - a \log \kappa_X)$ so that a value of D may be estimated for each sam-

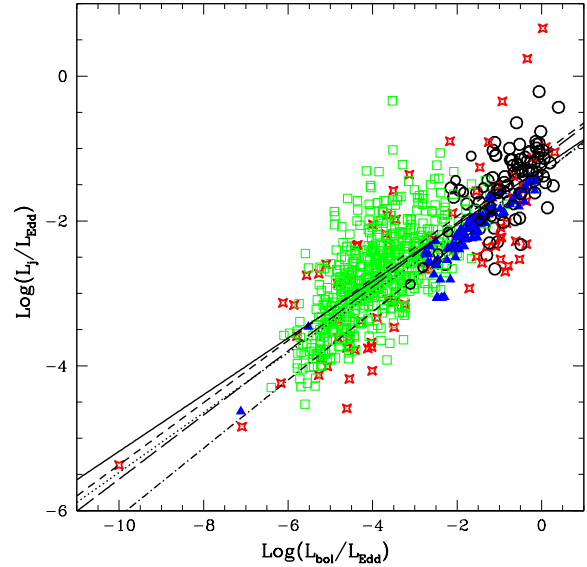


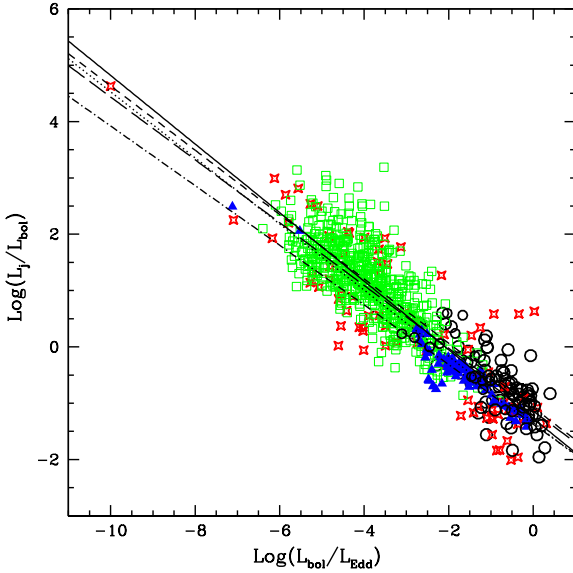
Figure 1. The log of the dimensionless beam power is shown versus the log of the dimensionless bolometric accretion disk luminosity for 576 LINERS (open green squares), 80 AGN (open red stars), 102 XRB measurements (solid blue triangles), and 97 powerful extended radio sources (open black circles). The best fit lines are: medium dashed line (576 LINERS); dotted line (80 AGN); dot-dash line (102 XRB); long-dashed line (97 FR II sources); and solid line (all 855 measurements). These symbols are used throughout the paper. Best fit parameters are listed in Table 2.

ple if an estimate of the value of B is available, given the values of C and $\log \kappa_X$ described above. Daly (2016) studied a sample of 97 powerful extended radio sources for which beam powers, bolometric luminosities, and Eddington luminosities were available and obtained a value of $B = -1.14 \pm 0.06$. It is easy to show that propagating the uncertainties of all parameters, the uncertainty of c has an insignificant impact on the uncertainty of D , so this term is not included in computing the uncertainty of D . Values of D thus obtained are listed in column (9) of Table 1.

Table 2. Best Fit Dimensionless Fundamental Plane (DFP) Parameters

(1) Sample	(2) N	(3) A	(4) B	(5) dispersion of DFP ^a	(6) dispersion of FP
NB16	576 LINERS	0.43 ± 0.02	-1.08 ± 0.08	0.47	0.73
M03	80 AGN + 36 XRB	0.45 ± 0.03	-0.94 ± 0.10	0.65	0.88
M03	80 AGN	0.41 ± 0.04	-1.34 ± 0.14	0.71	
D16	97 FRII AGN	0.44 ± 0.05	-1.14 ± 0.06	0.38	
S15	102 XRB	0.47 ± 0.02	-1.37 ± 0.04	0.19	
S15	102 XRB ($\kappa_X = 5$)	0.47 ± 0.02	-1.15 ± 0.04	0.19	

^a Obtained assuming all of the dispersion is due to $\log(L_j/L_{\text{Edd}})$ and decreases by the factor $1/\sqrt{2}$ if it is equally weighted between this parameter and $\log(L_{\text{bol}}/L_{\text{Edd}})$.

**Figure 2.** The log of the ratio of beam power to bolometric accretion disk luminosity is shown versus the log of the dimensionless bolometric luminosity for the sources shown in Fig. 1.

3 APPLICATIONS

To obtain and study L_j/L_{Edd} and $L_{\text{bol}}/L_{\text{Edd}}$ samples were selected from the list of NB16 in such a way as to avoid duplicate measurements of any given source while maintaining the integrity of each sample. The samples considered include the 576 LINERS presented by NB16, 80 AGN presented by Merloni et al. (2003), and the 102 measurements from black holes that are part of Galactic X-ray binary systems (XRB) presented by Saikia et al. (2015). The value of L_{bol} is obtained for each source using eq. (3) with the value of $\log \kappa_X$ given above (one additional value is considered for the XRB), black hole mass is converted to L_{Edd} with the relation listed above, and L_j is obtained using eq. (4) given the values of C and D listed in columns (2) and (9) of Table 1; a value of D is not available for the Saikia et al. (2015) fit that included XRB (see row 8 of Table 1), but the fit of NB16(1) has values of a and b that are consistent with those of Saikia et al. (2015) and this fit goes right through the XRB points, so the NB16(1) values of C and D are applied to that sample; in addition, a value of $\kappa_X = 5$ suggested by Saikia et al. (2015) is also considered for the XRB. All values of L_R are

scaled to 1.4 GHz using the conversion factors of NB16. In addition, 97 classical double radio sources from Daly (2016) are included; independent values of L_j , L_{bol} , and L_{Edd} are available for these sources. These samples allow a comparison between various types of sources.

Results obtained with these four samples and the combined sample are shown in Fig. 1 and are summarized in Table 2; the results shown in Fig. 1 are obtained for $\kappa_X \simeq 15$ for all sources, and the values of L_{bol} decrease by about a factor of 3 for the XRB for $\kappa_X \simeq 5$. All fits are unweighted. To estimate the dispersion of $y = \log(L_j/L_{\text{Edd}})$, σ_y , we assume that all of the dispersion in the fit is due to the uncertainty in y , and following Merloni et al. (2003) and Gültekin et al. (2009), we assume the uncertainty is the same for each point. Setting the reduced χ^2 to unity then provides an estimate of σ_y . If there are additional sources of uncertainty, such as that of $x = \log(L_{\text{bol}}/L_{\text{Edd}})$, then σ_y will decrease since the total dispersion $\sigma_T^2 = \sigma_y^2 + \sigma_x^2$. For example, if $\sigma_x = \sigma_y$, then the dispersion will decrease by a factor of $1/\sqrt{2}$ from the values listed in column (5) of Table 2. Compared with the values of the dispersion of the FP available for the samples studied, which are listed in column (6) of Table 2 when available, the dimensionless fundamental plane (DFP) described by eq. (2) has a smaller dispersion than the FP. This is another indication that eq. (2) provides a good description of the data. Given the value of the dispersion for each sample, the reduced χ^2 of all samples combined is fixed, and turns out to be 1.04 for $\kappa_X = 5$ for XRB, and 1.16 for $\log \kappa_X = 1.18$ for XRB, supporting the idea (Saikia et al. 2015) that the conversion factor κ_X is about three times larger for AGN than it is for XRB. Fig. 1 indicates that eq. (2) provides a good description of the data over about 10 orders of magnitude in $L_{\text{bol}}/L_{\text{Edd}}$, from about 10^{-10} to about 1, and over about 5.5 orders of magnitude in L_j/L_{Edd} , from about $10^{-5.5}$ to about 1. Interestingly, the relationship seems to remain valid all the way up to values of $L_{\text{bol}}/L_{\text{Edd}} \sim 1$. Within uncertainties, the relationship between the dimensionless parameters is the same for all types of sources studied including LINERS, AGN, XRB, and powerful classical double radio sources. In addition, the values of A indicated by fundamental plane parameters, listed in column (7) of Table 1, are consistent with those obtained by a direct fit to the data, listed in Table 2.

Equation (2) may be re-written as

$$\log\left(\frac{L_j}{L_{\text{bol}}}\right) = (A - 1) \log\left(\frac{L_{\text{bol}}}{L_{\text{Edd}}}\right) + B, \quad (6)$$

which may be interpreted as the efficiency of the beam power relative to accretion disk power as a function of dimensionless disk luminosity. It is interesting to consider the range of values of this parameter, and results obtained with the samples discussed above are shown in Fig. 2. Here $y = \log(L_j/L_{bol})$, and the dispersion of this parameter for each sample and for the combined sample is the same as those quoted in Table 2 for $y = \log(L_j/L_{Edd})$, and best fit values of the slope ($A - 1$), shown in Fig. 2, can easily be obtained from the values of A listed in Table 2.

Values of L_j/L_{bol} extend over about 7 orders of magnitude from about $10^{-2} - 10^5$ while the range of values, and the relationship between L_j/L_{bol} and L_{bol}/L_{Edd} is similar for all classes of objects studied. The transition from sources with $L_j > L_{bol}$, considered to be “jet dominated,” to those with $L_j < L_{bol}$, considered to be “disk dominated,” occurs at about $L_{bol}/L_{Edd} \sim (10^{-3} \text{ to } 10^{-2})$. This is consistent with previous results that find that “jet dominated” sources have low values of L_{bol}/L_{Edd} , while those that are “disk dominated” have high values of this parameter (e.g. see the summaries of Fender 2010; Yuan & Narayan 2014; and Heckman & Best 2014).

4 SUMMARY AND DISCUSSION

The fact that the FP of black hole activity is manifestly scale invariant suggests that it represents a relationship between the dimensionless beam power and the dimensionless bolometric luminosity of the black hole system. In section 2 it is shown that a dimensionless representation of the fundamental plane is consistent with detailed studies of the FP of black hole activity (see columns 2, 5, and 6 of Table 1). Given that eq. (1) may be written in the form of eq. (2), the value of A may be written in terms of best fit FP parameters a and b : $A = a/(a + b)$. In terms of understanding the physics of the sources and constraining models that describe the sources, A is of paramount importance since eq. (2) implies that $L_j \propto L_{bol}^A M^{(1-A)}$. All nine samples studied are consistent with a single value of A and yield a weighted mean value of 0.45 ± 0.02 (see column (7) of Table 1); this is consistent with the value of 0.44 ± 0.05 obtained independently by Daly (2016) for powerful extended radio sources. In addition, these results are consistent with those obtained by Fender, Gallo, & Jonker (2003), who find $L_j \propto L_X^{0.5}$.

Two equivalent forms of the DFP, given by eqs. (2) and (6), are studied directly using four data sets that include LINERS, AGN, XRB, and powerful classical double radio sources. All categories of source have consistent best fit values of A and B (see Figs. 1 and 2 and Table 2), and the DFP has a smaller dispersion than the FP, supporting the longstanding interpretation of the FP as arising from a relationship between the fundamental physical variables that describe black hole systems. This representation allows a study of the range of values of L_j/L_{Edd} , L_{bol}/L_{Edd} , and L_j/L_{bol} , and the relationships between these parameters. For the sources studied L_j/L_{Edd} ranges from about $10^{-5.5}$ to about 1; L_{bol}/L_{Edd} ranges from about 10^{-10} to about 1; and L_j/L_{bol} ranges from about 10^{-2} to about 10^5 . These results support the conclusion of previous studies that the sources transition from jet dominated to disk dominated, which is defined to occur at $L_j/L_{bol} \sim 1$, at a value of

$L_{bol}/L_{Edd} \sim (10^{-3} \text{ to } 10^{-2})$. Interestingly, the relationships between the dimensionless parameters L_j/L_{bol} or L_j/L_{Edd} and L_{bol}/L_{Edd} seem to remain valid over the full range of values of L_{bol}/L_{Edd} studied, including $L_{bol}/L_{Edd} \sim 1$. The values of A and B , particularly A , describe the physics of the sources and have implications for models of black hole systems. The fact that one dimensionless equation, eq. (2) or eq. (6), describes all sources, including sources that do not have compact radio emission, over such large ranges of dimensionless parameters, suggests that a common physical mechanism set primarily by L_{bol}/L_{Edd} regulates the beam power relative to the accretion disk power in these systems.

ACKNOWLEDGMENTS

Thanks are extended to Philip Best, David Nisbet, and an anonymous referee for helpful comments and suggestions which have significantly improved the paper. Daly would like to thank the Aspen Center for Physics for hosting the March 2016 meeting and the 2016 summer workshop on black hole physics where this work was discussed; in particular, thanks are extended to Norm Murray, Syd Meshkov, Pepi Fabbiano, Martin Elvis, Christine Jones, Bill Forman, Rosie Wyse, Rachel Webster, and Garth Illingworth for helpful conversations. This work was supported in part by Penn State University and performed in part at the Aspen Center for Physics which is support by National Science Foundation grant PHY-1066293.

REFERENCES

- Bonchi A., La Franca F., Melini G., Bongiorno A., & Fiore F., 2013, MNRAS, 429, 1970
- Daly, R. A. 2016, MNRAS 458, L24
- de Gasperin, F., Merloni, A., Sell, P., Best, P., Heinz, S., & Kauffmann, G. 2011, MNRAS, 415, 2910
- Falcke, H., Körding, E., & Markoff, S. 2004, A&A, 414, 895
- Fender, R. 2010, in The Jet Paradigm, Lecture Notes in Physics. Springer-Verlag Berlin, 794, 115
- Fender, R. P., Gallo, E., & Jonker, P. G. 2003, MNRAS, 343, L99
- Gültekin K., Cackett E. M., Miller J. M., Di Matteo T., Markoff S., & Richstone D. O., 2009, ApJ, 706, 404
- Heckman, T. M., & Best, P. N. 2014, ARA&A, 52, 589
- Heinz S. & Sunyaev R. A., 2003, MNRAS, 343, L59
- Ho, L. C. 2009, ApJ, 699, 626
- Körding E. G., Falcke H., & Corbel S., 2006, A&A, 456, 439
- Körding, E. G., Fender, R. P., & Migliari, S. 2006, MNRAS, 369, 1451
- Marconi, A., Risaliti, G., Gilli, R., Hunt, L. K., Maiolino, R., & Salvati, M. 2004, MNRAS, 351, 169
- Merloni A. & Heinz S., 2007, MNRAS, 381, 589
- Merloni A., Heinz S., & di Matteo T., 2003, MNRAS, 345, 1057
- Nisbet, D. M., & Best, P. N. 2016, MNRAS, 455, 2551
- Saikia P., Körding E., & Falcke H., 2015, MNRAS, 450, 2317
- Willott, C. J., Rawlings, S., Blundell, K. M., & Lacy, M. 1999, MNRAS, 309, 1017
- Yuan, F., & Narayan, R. 2014, ARA&A, 52, 529
- Yuan, Z., & Wang, J. 2012, ApJ, 744:84, 1